Issues in Modal Identification of Flexible Structures

H. Baruh* and J. Boka†
Rutgers University, New Brunswick, New Jersey 08903

Issues associated with implementation of modal parameter identification procedures that are based upon discretized models are discussed. The interest lies in methods where the identification is carried out as a correction process on a postulated model generated by using erroneous system parameters. It is shown that the identification approach loses its accuracy because a discretized model has to be used to represent the structure and because extraction of the modal information from the sensors' output introduces contamination from the unmodeled modes. The level of this inaccuracy is investigated qualitatively and quantitatively.

I. Introduction

THIS paper is concerned with implementation details associated with modal parameter identification methods for structural systems. The interest lies in investigating problems such as the use of a discrete model when the actual model is continuous, the errors associated with extraction of modal coordinates from the system output, and the inaccuracies in the underlying assumptions on which the identification procedure is based. All these effects reduce the accuracy with which the system can be identified. This reduction of accuracy is investigated qualitatively and quantitatively by considering the identification method proposed in Ref. 1.

The field of parameter identification is a large one, where the present state of the art has been surveyed frequently (e.g., Refs. 2–5). Structural identification methods can be broadly classified into time-domain or frequency-domain categories.[5] Another characterization of existing work is by what is identified. In identifying mass and stiffness properties of a structure, some approaches consider identification of these parameters directly from the system response.[6–9] In Refs. 6 and 7 continuous models are used, and in Refs. 8 and 9 spatially discretized models are considered. Other approaches consider identification of the eigensolution first.[10–12] Identification of the mass and stiffness properties is then carried out using this identified eigensolution,[13–17] or previously known modal information. Identification of external excitations from the time history of the system modes has been considered in Ref. 18.

Implementation of an identification scheme is not complete until the approach is tested under a variety of circumstances and actual experiments are conducted. In this paper, we examine several implementation issues associated with modal identification methods and in particular with methods where the identification is carried out as a correction process on a postulated model, such as in Ref. 1. Factors that contaminate the identification include errors associated with the extraction of the modal coordinates from the system output and use of a discretized model. To extract modal quantities from the system output, two approaches emerge. One is the use of modal filters and the other is observers.[19] A comparison between the two indicates that modal filters are more desirable to use than observers,[19,20] so that the approach here will be to use modal filters.

Modal filtering is based on interpolating the sensors' output to get a spatially distributed estimate of the system profile, and then using the expansion theorem.[19] Because discrete sensors are used, the extracted modal coordinates are not the exact ones, and they are contaminated by other modal coordinates.

When a discretized model is used to analyze a continuous system, there exist errors associated with the discretization, except for very low modes. These errors, when combined with the output of the modal filters, contaminate the modal response that is extracted from the actual measurements. The effects of such contamination are analyzed. Also, because the order of the discretized model is generally very large, one can opt to identify a subset of the modes in the model. The unidentified residual modes further contaminate the accuracy of the modes that are identified. Ultimately, one has to make a decision as to whether to identify fewer modes, where the errors in filtering and discretization are small, or to identify a larger number of modes, where the effects of discretization errors are more significant.

II. Equations of Motion

Consider a self-adjoint distributed structure whose behavior is described by

$$m(x)\ddot{u}(x,t) + Lu(x,t) = f(x,t) \tag{1}$$

where $u(x,t)$ is the displacement at x at time t, L is a stiffness operator, $m(x)$ is the mass distribution, and $f(x,t)$ denotes the external forces.[21] Using standard methods of analysis, one can arrive at the modal equations in the form

$$\ddot{\eta}_r(t) + \lambda_r \eta_r(t) = f_r(t), \qquad r = 1, 2, \ldots \tag{2}$$

where λ_r are the eigenvalues, related to the natural frequencies by $\lambda_r = \omega_r^2$, and $\eta_r(t)$ and $f_r(t)$ are modal coordinates and modal forces, respectively, related to the displacement $u(x,t)$ and forcing $f(x,t)$ by the expansion theorems

$$u(x,t) = \sum_{r=1}^{\infty} \phi_r(x)\eta_r(t), \qquad \eta_r(t) = [\phi_r(x),\ m(x)u(x,t)]$$

$$f(x,t) = \sum_{r=1}^{\infty} m(x)\phi_r(x)f_r(t), \qquad f_r(t) = [\phi_r(x),\ f(x,t)] \tag{3}$$

in which $[a,b] = \int ab\ dx$, and $\phi_r(x)$ are the system eigenfunctions. The eigenfunctions can be rendered mutually orthonor-

Received April 4, 1988; presented as Paper 88-2409 at the AIAA/ASME/ASCE/AHS/ASC 29th Structures, Structural Dynamics, and Materials Conference, Williamsburg, VA, April 8–10, 1988; revision received July 8, 1989; accepted for publication July 10, 1989.

*Associate Professor, Department of Mechanical and Aerospace Engineering. Member AIAA.

†Graduate Fellow, Department of Mechanical and Aerospace Engineering; currently Control System Design Engineer, GE Astro Space, King of Prussia, PA 19406.

mal using

$$[\phi_r(x),\ m(x)\phi_s(x)] = \delta_{rs}, \qquad [\phi_r(x),\ L\phi_s(x)] = \omega_r^2\delta_{rs}$$

$$(r,s = 1,\ 2,\ \ldots)$$

If the excitation $f(x,t)$ is in the form of k discrete forces $F_i(t)$ acting at $x_i (i = 1, 2, \ldots, k)$, the modal forces have the form

$$f_r(t) = [\phi_r(x),\ f(x,t)] = \int \phi_r(x) \sum_{i=1}^{k} F_i(t)\delta(x - x_i)\, dx$$

$$= \sum_{i=1}^{k} \phi_r(x_i)F_i(t) \tag{4}$$

A closed-form solution of the governing equation is, for most of the time, impossible to obtain, so that we seek an approximate solution using spatial discretization. To this end, consider the equation

$$u(x,t) = \sum_{r=1}^{n} \psi_r(x)a_r(t) \tag{5}$$

where $\psi_r(x)$ are admissible functions (global or local),[21] and $a_r(t)$ are undetermined coefficients. It follows that one ends with a discretized set of equations of order n

$$M\ddot{a}(t) + Ka(t) = BF(t) \tag{6}$$

in which the entries of the mass and stiffness matrices M and K have the form

$$m_{ij} = [\psi_i(x),\ m(x)\psi_j(x)], \qquad k_{ij} = [\psi_i(x),\ \psi_j(x)]^*$$

where the starred square brackets denote an energy inner product.[21] B is the actuator influence matrix and

$$F(t) = [F_1(t),\ F_2(t),\ \ldots,\ F_k(t)]^T$$

The eigenvalue problem associated with Eq. (6) yields a set of n eigenvalues $\Lambda_1, \Lambda_2, \ldots, \Lambda_n$, and corresponding eigenvectors $u_r (r = 1, 2, \ldots, n)$. The eigenvalues are approximations to the squares of the natural frequencies ω_r^2 and the eigenvectors can be used to approximate the eigenfunctions $\phi_r(x)$ as

$$\theta_r(x) = u_r^T\psi(x), \qquad r = 1,\ 2,\ \ldots,\ n \tag{7}$$

where $\theta_r(x)$ are what we will refer to as the discretized eigenfunctions and $\psi(x) = [\psi_1(x), \psi_2(x), \ldots, \psi_n(x)]^T$. The eigenvectors are orthogonal with respect to the mass and stiffness matrices and they can be normalized as

$$u_r^T M u_s = \delta_{rs}, \qquad u_r^T K u_s = \Lambda_r\delta_{rs} \qquad (r,s = 1,\ 2,\ \ldots,\ n)$$

or

$$U^T M U = I, \qquad U^T K U = \Lambda$$

where $U = [u_1,\ u_2,\ \ldots,\ u_n]$ is the modal vector and Λ is a diagonal matrix containing the eigenvalues. Using the expansion theorem

$$u(x,t) = \sum_{r=1}^{n} \theta_r(x)q_r(t), \qquad q_r(t) = [\theta_r(x),\ m(x)u(x,t)]$$

$$r = 1,\ 2,\ \ldots,\ n \tag{8}$$

which is equivalent to $a(t) = Uq(t)$, where

$$q(t) = [q_1(t),\ q_2(t),\ \ldots,\ q_n(t)]^T$$

are modal coordinates of the discretized system. The modal equations associated with the discretized system can be obtained as

$$\ddot{q}_r(t) + \Lambda_r q_r(t) = h_r(t), \qquad r = 1,\ 2,\ \ldots,\ n \tag{9}$$

where $h_r(t)$ are associated modal forces obtained by

$$h_r(t) = [\theta_r(x),\ f(x,t)] \qquad (r = 1,\ 2,\ \ldots,\ n)$$

Consider next the discretized equations of motion in the presence of parameter uncertainties. It is assumed that the general form of the equations of motion and the geometric boundary conditions are known, but the parameters contained in the mass and stiffness operators are not known. Postulating these erroneous operators by $m'(x)$ and L', and using Eq. (5), we arrive at the discretized equations of motion of the postulated system as

$$M'\ddot{a}(t) + K'a(t) = B'F(t) \tag{10}$$

where the primes denote that the matrices are based on erroneous parameters.

The eigensolution associated with the erroneous model is in the form of n eigenvalues $\Lambda_1', \Lambda_2', \ldots, \Lambda_n'$, and corresponding eigenvectors $v_r (r = 1,\ 2,\ \ldots,\ n)$. The eigenvectors can be used to approximate the eigenfunctions of the erroneous system as

$$\theta_r'(x) = v_r^T\psi(x), \qquad r = 1,\ 2,\ \ldots,\ n \tag{11}$$

Similar to Eqs. (8) and (9), the orthogonality conditions, expansion theorem, and postulated modal equations become

$$v_r^T M' v_s = \delta_{rs}, \qquad v_r^T K' v_s = \Lambda_r'\delta_{rs}, \qquad r,s = 1,\ 2,\ \ldots,\ n$$

$$u(x,t) = \sum_{r=1}^{n} \theta_r'(x)q_r'(t), \qquad q_r'(t) = [\theta_r'(x),\ m'(x)u(x,t)]$$

$$\ddot{q}_r'(t) + \Lambda_r'q_r'(t) = h_r'(t), \qquad h_r'(t) = [\theta_r'(x),\ f(x,t)] \tag{12}$$

with terms taking their obvious meaning.

We wish to explore the relations between the eigenfunctions and modal coordinates associated with the actual, discretized, and postulated systems of equations. First, consider the actual and discretized systems. Because the actual eigenfunctions constitute a complete set, one can express the eigenfunctions of the discretized system as

$$\theta_r(x) = \sum_{s=1}^{\infty} d_{rs}\phi_s(x) = d_r^T\phi(x), \qquad r = 1,\ 2,\ \ldots,\ n \tag{13}$$

where

$$\phi(x) = [\phi_1(x),\ \phi_2(x),\ \ldots]^T$$

and

$$d_r = [d_{r1},\ d_{r2},\ \ldots]^T \qquad (r = 1,\ 2,\ \ldots,\ n)$$

The coefficients d_{rs} can be obtained by multiplying Eq. (13) by $m(x)\phi_s(x) (s = 1, 2, \ldots,)$ and integrating, which yields

$$d_{rs} = [m(x)\phi_s(x),\ \theta_r(x)] \qquad (r = 1,\ 2,\ \ldots,\ n;\ s = 1,\ 2,\ \ldots)$$

It can be shown that $d_r^T d_s = \delta_{rs}$.

Using Eq. (13) and the expansion theorems, the relationship between the actual modal coordinates and discretized modal coordinates becomes

$$q_r(t) = \sum_{s=1}^{\infty} d_{rs}\eta_s(t) = d_r^T\eta(t), \qquad r = 1,\ 2,\ \ldots,\ n \tag{14}$$

where $\eta(t) = [\eta_1(t),\ \eta_2(t),\ \ldots]^T$. Equation (14) can also be expressed in matrix form as $q(t) = D\eta(t)$, where $q(t)$ was defined earlier and $D = [d_1,\ d_2,\ \ldots,\ d_n]^T$. Note that the modal coordinates $q_r(t)$ considered in Eq. (14) are not the coordinates obtained by integrating the discretized equations of motion. They are coordinates obtained by applying the expansion theorem, Eq. (8).

Naturally, as more terms in the expansion of Eq. (13) are taken, the difference between the actual and discretized eigenfunctions should get smaller. To illustrate this, we introduce the error function

$$\epsilon_r(x) = \phi_r(x) - \theta_r(x), \qquad (r = 1, 2, \ldots, n)$$

which leads to

$$[\epsilon_r(x),\ m(x)\epsilon_r(x)] = [\phi_r(x),\ m(x)\phi_r(x)] + [\theta_r(x),\ m(x)\theta_r(x)]$$

$$-2[\phi_r(x),\ m(x)\theta_r(x)] = 2(1 - d_{rr}), \quad r = 1, 2, \ldots, n \tag{15}$$

Similarly, by taking the energy inner product of $\epsilon_r(x)$ we obtain

$$[\epsilon_r(x),\ \epsilon_r(x)]^* = [\phi_r(x),\ \phi_r(x)]^* + [\theta_r(x),\ \theta_r(x)]^*$$

$$-2[\theta_r(x),\ \phi_r(x)]^* = \lambda_r + \Lambda_r - 2d_{rr}\lambda_r, \qquad r = 1, 2, \ldots, n \tag{16}$$

Defining the error in the rth eigenvalue as $E_r = \Lambda_r - \lambda_r$, and combining Eqs. (15) and (16) we obtain the relation

$$[\epsilon_r(x),\epsilon_r(x)]^* - \lambda_r[\epsilon_r(x),\ m(x)\epsilon_r(x)] = \Lambda_r - \lambda_r = E_r$$

$$r = 1, 2, \ldots, n \tag{17}$$

which can be regarded as a measure of the discretization error. Because as the model order is increased by virtue of the inclusion principle[21] E_r becomes smaller, one can heuristically conclude that d_{rr} should approach unity. Because

$$\sum_{s=1}^{\infty} d_{rs}^2 = 1$$

as d_{rr} becomes larger the off-diagonal terms get smaller.

We next relate the discretized and postulated models. The associated modal matrices U and $V(V = [v_1, v_2, \ldots, v_n])$ can be related by

$$U = VC \tag{18}$$

where the entries of C are $c_{rs} = v_r^T M' u_s$ or $C = V^T M' U$. It is this matrix C that needs to be identified in order to arrive at the actual model.

When we introduce the notation $C = [c_1, c_2, \ldots, c_n]^T$ and $C^{-T} = \bar{C} = [\bar{c}_1, \bar{c}_2, \ldots, \bar{c}_n]^T$, it follows that the postulated eigenfunctions and modal coordinates are related to the discretized ones by

$$\theta_r'(x) = \bar{c}_r^T\theta(x), \qquad q_r'(t) = c_r^T q(t), \qquad r = 1, 2, \ldots, n \tag{19}$$

We are now in a position to relate the actual and postulated modal quantities. Using Eqs. (12–14), (18), and (19), we obtain

$$q_r'(t) = c_r^T q(t) = c_r^T D\eta(t), \quad \text{or} \quad q'(t) = Cq(t) = CD\eta(t)$$

$$\theta_r'(x) = \bar{c}_r^T\theta(x) = \bar{c}_r^T D\phi(x), \quad \text{or} \quad \theta'(x) = \bar{C}\theta(x) = \bar{C}D\phi(x) \tag{20}$$

The above equations indicate the relationship between the actual eigensolution and the discretized model solution in the presence of parameter uncertainties. The parameter uncertainty and discretization errors are represented by the matrices C and D, respectively. In control systems these matrices tend to contaminate the performance of the control design. In parameter identification procedures, one can opt to identify the matrix C. But, because the model used is derived from spatial discretization, existence of the matrix D will degrade the results of the identification.

III. Reduced-Order Model and Modal Coordinate Extraction

When a discretized model for a structure is constructed, the order of the model far exceeds the number of modes of interest, especially when the discretization is based on the finite element method. In such cases, a reduced-order model needs to be constructed from the discretized model. Denoting the number of modes of interest by m (denoted by the subscript M), and partitioning the modal quantities into m monitored and $n - m$ residuals (denoted by the subscript R) in the form

$$q(t) = \begin{vmatrix} q_M(t) \\ q_R(t) \end{vmatrix}, \qquad U = [U_M \mid U_R]$$

$$\theta(x) = \begin{vmatrix} \theta_M(x) \\ \theta_R(x) \end{vmatrix}, \qquad \lambda = \left|\begin{array}{c|c} \Lambda_M & 0 \\ \hline 0 & \Lambda_R \end{array}\right| \tag{21}$$

and considering Eqs. (6–9) we obtain the reduced-order equations

$$\ddot{q}_M(t) + \Lambda_M q_M(t) = U_M^T BF(t) = N_M(t) \tag{22}$$

One then performs the identification using $q_M(t)$ as the configuration vector. To investigate the effect of using a reduced-order model, we partition the postulated modal coordinates, eigenfunctions, and matrices C and $\bar{C}$ as

$$q'(t) = \begin{vmatrix} q_M'(t) \\ q_R'(t) \end{vmatrix}, \qquad \theta'(x) = \begin{vmatrix} \theta_M'(t) \\ \theta_R'(t) \end{vmatrix}$$

$$C = \left|\begin{array}{c|c} C_{MM} & C_{MR} \\ \hline C_{RM} & C_{RR} \end{array}\right|, \qquad \bar{C} = \left|\begin{array}{c|c} \bar{C}_{MM} & \bar{C}_{MR} \\ \hline \bar{C}_{RM} & \bar{C}_{RR} \end{array}\right| \tag{23}$$

which yields for the monitored modes and eigenfunctions

$$q_M'(t) = C_{MM}q_M(t) + C_{MR}q_R(t)$$

$$\theta_M'(x) = \bar{C}_{MM}\theta_M(x) + \bar{C}_{MR}\theta_R(x) \tag{24}$$

The problem with dealing with Eqs. (24) instead of the full state is that the transformation matrix found by the identification process between $q_M(t)$ and $q_M'(t)$ will not be C_{MM}, but another matrix that is contaminated by the contribution of the residual modes.

We next consider the extraction of the modal quantities from the system output. To this end, use will be made of modal filters.[19]

Modal filtering is based on the idea of interpolating and extrapolating the sensor output to obtain a spatially distributed estimate of the system displacement (or velocity or acceleration) and then using the expansion theorem to extract the modal coordinates. The estimated distributed profile $\hat{u}(x,t)$ can be calculated as

$$\hat{u}(x,t) = \sum_{j=1}^{\ell} u(x_j,t)G(x,x_j) \tag{25}$$

where x_j denotes the location of the sensors $(j = 1, 2, \ldots, \ell)$ and $G(x,x_j)$ are interpolation or extrapolation functions, in which the time and space dependency are separate. Introducing Eq. (25) into the expansion theorem we obtain expressions for the extracted modal coordinates, defined[19] by

$$\hat{q}_r(t) = [\hat{u}(x,t),m(x)\theta_r(x)] = \sum_{j=1}^{\ell} g_{rj}u(x_j,t), \quad r = 1, 2, \ldots \tag{26}$$

in which

$$g_{rj} = [G(x,x_j),m(x)\theta_r(x)] \qquad (j = 1, 2, \ldots, \ell;\ r = 1, 2, \ldots)$$

are modal filter gains.[20] Note that these gains are computed off-line, prior to the identification process.

The accuracy of modal filtering depends on the number of sensors and types of interpolation functions. Noting that the sensor measurements $y_j(t)$ are

$$y_j(t) = \sum_{s=1}^{n} \theta_s(x_j) q_s(t) + n_j(t), \qquad j = 1, 2, \ldots, \ell \tag{27}$$

where $n_j(t)$ denotes measurement noise, and introducing the extracted modal coordinate vector

$$\hat{q}_M(t) = [\hat{q}_1(t), \hat{q}_2(t), \ldots, \hat{q}_m(t)]^T$$

we can combine Eqs. (26) and (27) into

$$\hat{q}_M(t) = GH_M q_M(t) + GH_R q_R(t) + Gn(t) \tag{28}$$

where the entries of G are

$$g_{rj}(r = 1, 2, \ldots, m; j = 1, 2, \ldots, \ell)$$

and

$$H_M(i,j) = \theta_j(x_i), \qquad H_R(i,j) = \theta_{m+j}(x_i)$$

The objective is to select m, ℓ, and the types of sensors such that GH_M approaches an identify matrix and GH_R approaches a null matrix. It is shown in Ref. 18 that if Rayleigh-Ritz type modal filters are used, GH_M becomes exactly an identity matrix, but the elements of GH_R are not considered. Actually, such a relation can be obtained without considering modal filters at all. Introducing the vector

$$y(t) = [y_1(t), y_2(t), \ldots, y_\ell(t)]^T$$

and considering Eq. (27) we can write

$$y(t) = H_M q_M(t) + H_R q_R(t) + n(t) \tag{29}$$

and if the number of sensors is equal to the number of monitored modes, $m = \ell$, and ignoring the residual modes, we invert Eq. (29) as

$$\hat{q}_M(t) = H_M^{-1} y(t) \tag{30}$$

which results in

$$\hat{q}_M(t) = q_M(t) + H_M^{-1} H_R q_R(t) + H_M^{-1} n(t) \tag{31}$$

This approach gives good results as long as the sensors are distributed very evenly around the structure. In the presence of modeling errors, Eqs. (25-31) are still valid, as long as all modal quantities are replaced by primes. That is, having parameter uncertainties does not affect the nature of the modal coordinate extraction. This is one reason why modal filters are preferable to other types of modal coordinate extraction.

We next find a relationship between $q_M(t)$ and $\hat{q}'_M(t)$. Combining Eqs. (24) and (28) we obtain

$$q'_M(t) = (G' H'_M C_{MM} + G' H'_R C_{RM}) q_M(t) + (C' H'_M C_{MR} + G' H'_R C_{RR}) q_R(t) + G' n(t) \tag{32}$$

We observe from the equation that one faces a dilemma when determining the number of monitored modes given a certain number of sensors. If the number of monitored modes is left as a small number, $G' H'_M$ will be almost an identity matrix and $G' H'_R$ will approach zero. On the other hand, C_{RM} will have a substantial contribution to the first term in Eq. (32). If the number of monitored modes is increased, $G' H'_M$ will lose its accuracy and $G' H'_R$ will have larger entries, but the contribution of C_{RM} will be smaller. The ideal case is, of course, to have a very large number of sensors, so that the contamination effects in extraction of modal coordinates become negligible.

We next consider that the model at hand is not discrete, but that it is discretized. That is, up to now it was assumed that the actual modal coordinates were $q_r(t)$, belonging to the spatially discretized model. However, the modal coordinates associated with the structure are related to the discretized coordinates by Eq. (14). Introducing the partitions

$$\eta(t) = \left| \begin{matrix} \eta_M(t) \\ \hline \eta_R(t) \end{matrix} \right|, \qquad D = \left| \begin{matrix} D_{MM} & D_{MR} \\ \hline D_{RM} & D_{RR} \end{matrix} \right| \tag{33}$$

we can express Eqs. (14) as

$$q_M(t) = D_{MM} \eta_M(t) + D_{MR} \eta_R(t)$$

$$q_R(t) = D_{RM} \eta_M(t) + D_{RR} \eta_R(t) \tag{34}$$

which, when introduced into Eq. (32), give the exact relationship between the extracted postulated modal coordinates and the actual modal coordinates in the form

$$\begin{aligned} \hat{q}'_M(t) = {} & [(G' H'_M C_{MM} + G' H'_R C_{RM}) D_{MM} \\ & + (G' H'_M C_{MR} + G' H'_R C_{RR}) D_{MR}] \eta_M(t) \\ & + [(G' H'_M C_{MM} + G' H'_R C_{RM}) D_{RM} \\ & + (G' H'_M C_{MR} + G' H'_R C_{RR}) D_{RR}] \eta_R(t) + G' n(t) \end{aligned} \tag{35}$$

It is clear that use of a discretized model will contaminate the results of the identification further. We will quantitatively examine the effects of such errors in Sec. V within the context of the identification method developed in Ref. 1.

IV. Identification Procedure

To illustrate the effects of spatial discretization, reduced-order modeling, and discrete sensors, we will use the identification procedure outlined in Ref. 1, which assumes a linear, undamped model and that the mass properties are known accurately. Considering the mass properties to be known is a reasonable assumption, because mass is a quantity that can be directly measured, whereas stiffness is not. We will examine the validity of assuming an undamped model within the context of a numerical example later on in this paper. Note that there are methods that identify damping in structures (e.g., Refs. 9, 11, and 17).

The discretized equations of motion of the postulated system then assume the form

$$M\ddot{a}(t) + K' a(t) = B' F(t) \tag{36}$$

It is shown in Ref. 1 that for models of this form the transformation matrix C becomes unitary, and the relationship between the modal matrices U and V has the form

$$U = VC, \qquad V = UC^T \tag{37}$$

Furthermore, $C = \bar{C}$ and $c_i = \bar{c}_i (i = 1, 2, \ldots, n)$.

The procedure in Ref. 1 is described in terms of an actual and a postulated discretized system. We assume that Eq. (6) is the exact equation of motion and Eq. (36) the postulated equations of motion. The objective is to transform the modal vectors associated with the erroneous model [Eq. (36)] so that they match their correct values. The procedure considered in Ref. 1 is to iteratively perform this transformation. Denoting the modal matrix associated with the erroneous model by $V = U_1$ and $C = C_1$, Eq. (18) can be expressed as

$$U = U_1 C_1 \tag{38}$$

In the identification procedure, a unitary transformation R_i is used at each step resulting in the updated matrices

$$U_2 = U_1R_1, \qquad U_3 = U_2R_2, \ldots, U_{\rho+1} = U_\rho R_\rho$$
$$C_2 = R_1^T C_1, \qquad C_3 = R_2^T C_2, \ldots, C_{\rho+1} = R_\rho^T C_\rho \tag{39}$$

where ρ is the total number of iterations to identify the actual system, so that $U_{\rho+1} = U$ and $C_{\rho+1} = I$. It follows that $C = C_1 = R_1R_2 \ldots R_\rho$ (Ref. 1). It is not necessary to calculate C explicitly.

The unitary transformation matrices R_i (also referred to as rotation matrices[22]) are selected such that at each iteration two modal vectors are transformed, and the other modes are unaffected, which leads to

$$R_{ijj} = 1, \qquad j = 1, 2, \ldots, n, \quad j \neq r, \quad j \neq s$$
$$R_{irr} = R_{iss} = \cos\theta_{irs}, \quad R_{irs} = -\sin\theta_{irs}, \quad R_{isr} = \sin\theta_{irs} \tag{40}$$
$$R_{ipq} = 0 \qquad p \neq q; \quad p \neq r \text{ when } q = s, \; q \neq r \text{ when } p = s$$

where θ_{irs} is the rotation angle between the rth and sth modal vectors at the ith iteration.

To transform all possible pairs of modal vectors $n(n-1)/2$ rotations need to be performed, which is referred to as a sweep.[21] A number of criteria can be used to select the rotation angles θ_{irs} (Ref. 22). One approach is to use the transient response, assuming that the external excitation is known.[1] The response of a certain mode (assuming that the discretized model is exact) can be expressed as

$$q_r(t) = q_{rh}(t) + q_{rp}(t), \qquad r = 1, 2, \ldots, n \tag{41}$$

where

$$q_{rh}(t) = 2A_r \cos(\bar{\omega}_r t - \sigma_r), \qquad r = 1, 2, \ldots, n \tag{42}$$

is the homogeneous solution, in which A_r and σ_r depend on the initial conditions and $\bar{\omega}_r^2 = \Lambda_r (r = 1, 2, \ldots, n)$. The Fourier transforms of the modal responses then become

$$Q_r(\omega) = \int_{-\infty}^{\infty} e^{i\omega t} q_r(t)\, dt$$
$$= (A_r \cos\sigma_r + iA_r \sin\sigma_r)\delta(\omega - \bar{\omega}_r) + P_r(\omega)$$
$$r = 1, 2, \ldots, n \tag{43}$$

where $P_r(\omega)$ denotes the frequency spectrum of the particular solution. One needs to deal only with the positive values of ω.

In the presence of parameter uncertainties, the spectrum of the postulated modal coordinates becomes

$$Q_r'(\omega) = \int_{-\infty}^{\infty} e^{-i\omega t} q_r'(t)\, dt$$
$$= \sum_{s=1}^{n} c_{rs} \int_{-\infty}^{\infty} e^{-i\omega t} q_s(t) = \sum_{s=1}^{n} c_{rs} Q_s(\omega)$$
$$= \sum_{s=1}^{n} c_{rs}(A_s \cos\sigma_s + iA_s \sin\sigma_s)\delta(\omega - \bar{\omega}_s)$$
$$+ \sum_{s=1}^{n} c_{rs} P_s(\omega), \qquad r = 1, 2, \ldots, n \tag{44}$$

with c_{rs} denoting the entries of C. Equation (44) indicates that the frequency spectra is scattered with peaks. The rotation criterion is then selected such that the number of peaks in the frequency spectra of the postulated modal coordinates is minimized. Introducing the terms

$$\mathrm{Re}_{rs} = c_{rs}A_s \cos\sigma_s, \quad \mathrm{Im}_{rs} = c_{rs}A_s \sin\sigma_s, \qquad r = 1, 2, \ldots, n$$

and considering that the sums of the amplitudes of the peaks

$$\sum_{r=1}^{n} \|(A_r \cos\sigma_r + iA_r \sin\sigma_r)\|$$
$$= \sum_{r=1}^{n} \sum_{s=1}^{n} \|c_{rs}(A_s \cos\sigma_s + iA_s \sin\sigma_s)\| \tag{45}$$

are invariant under a unitary transformation,[1] the rotation angles are chosen such that in a $r-s$ transformation the resulting Re_{rr}, Im_{rr}, Re_{ss}, Im_{ss} terms are maximized and Re_{rs}, Re_{sr}, Im_{rs}, Im_{sr} are minimized. The rotation angle θ_{irs} then becomes[1]

$$\theta_{irs} = \tfrac{1}{2} \tan^{-1}(2Z/X - Y) \tag{46}$$

in which

$$X = \mathrm{Re}_{rr}^2 + \mathrm{Im}_{rr}^2 + \mathrm{Re}_{ss}^2 + \mathrm{Im}_{ss}^2$$
$$Y = \mathrm{Re}_{sr}^2 + \mathrm{Im}_{sr}^2 + \mathrm{Re}_{rs}^2 + \mathrm{Im}_{rs}^2$$
$$Z = \mathrm{Re}_{rr}\mathrm{Re}_{sr} + \mathrm{Im}_{rr}\mathrm{Im}_{sr} - \mathrm{Re}_{rs}\mathrm{Re}_{ss} - \mathrm{Im}_{rs}\mathrm{Im}_{ss} \tag{47}$$

As stated before, other criteria can also be used when determining the rotation angle, such as the steady-state response.[22] The identification procedure continues until all rotation angles are lower than a prescribed threshold value, or until a maximum number of sweeps is exceeded. Note that the Fourier transform of the modal coordinates needs to be calculated only once, before the identification begins. Also, throughout the identification process, no equations are integrated. Only the system measurements are linearly transformed. Additional details about the identification process can be found in Ref. 1.

V. Illustrative Examples

As an illustration of the implementation problems associated with identification, we consider the axial vibration of a tapered rod of length L fixed at one end and free at the other. The equation of motion and boundary conditions are

$$m(x)\frac{\partial^2 u(x,t)}{\partial t^2} = \frac{\partial[EA(x)\partial u(x,t)]}{\partial x} + f(x,t)$$
$$u(0,t) = 0 \qquad \left.\frac{\partial u(x,t)}{\partial x}\right|_{x=L} = 0 \tag{48}$$

where $m(x)$ and $EA(x)$ are the mass and stiffness distributions, respectively, having the form

$$m(x) = 2m(1 - x/L), \qquad EA(x) = 2EA(1 - x/L) \tag{49}$$

The reason why this model is chosen is because it lends itself to a closed-form eigensolution, which can be shown to be

$$\phi_r(x) = J_0(\beta_r L[1 - x/L]) \qquad (r = 1, 2, \ldots)$$

where J_0 is the Bessel function of order zero, and β_r are the roots of $J_0(\beta_r L) = 0$, so that the actual response can be obtained. Also the natural frequencies are close to each other, which increases the significance of the modes that are not monitored.

First, we construct an approximate solution by spatial discretization. To this end, we will use two types of trial functions.

First set:

$$\psi_r(x) = \sin\frac{(2r-1)\pi x}{2L}$$

Second set:

$$\psi_r(x) = T_r(x/L) \qquad r = 1, 2, \ldots, n \tag{50}$$

The first set is the eigensolution of a bar of uniform cross-section, and the second set are Chebyshev polynomials, which lose their desirability after the first few modes.

Next, we consider parameter uncertainties. We assume the same mass distribution as in Eq. (49), where m is chosen as $m = 1$, and postulate the system stiffness as $EA(x) = 1 - (x/L)^2$, where the actual stiffness is $2(1 - x/L)$. We conduct the identification for various cases. The sensor measurements are contaminated by noise in the form

$$y_j(t) = u(x_j,t)[1 + R], \qquad j = 1, 2, \ldots, \ell \tag{51}$$

where $y_j(t)$ denotes the sensor measurements and R is a uniform random variable with the distribution $[-0.05, 0.05]$. It should be noted that the identification procedure was carried out using velocity and acceleration measurements as well. There was no visible change or trend of a change in the accuracy of the identification. The simulated measurements were transformed into the frequency domain by a fast Fourier transform.[23] The sensors were placed evenly, at the locations $x_j = jL/\ell + 1$, $j = 1, 2, \ldots, \ell$.

To examine the accuracy of the identification, an error coefficient is introduced as [note similarity with Eq. (15)]

$$e_r = [\delta_r(x), m(x)\delta_r(x)], \qquad r = 1, 2, \ldots, n \tag{52}$$

where $\delta_r(x)$ is the difference between the actual and identified eigenfunctions. Denoting the identified eigenfunctions by $\gamma_r(x)$, so that $\delta_r(x) = \phi_r(x) - \gamma_r(x)$, the error coefficients e_r can be shown to be

$$e_r = 2 - 2[\gamma_r(x), m(x)\phi_r(x)], \qquad r = 1, 2, \ldots, n \tag{53}$$

It can easily be demonstrated that e_r are always positive. We consider implementation of the identification procedure for varying cases of discretization, modal filtering, and model reduction. The accuracy of the identification is monitored by plotting the error coefficients e_r. The following cases are considered.

Case 1

The actual model is assumed to be the discretized one (using the first set of trial functions). Both the postulated and actual systems are of the same order, $n = 15$. Also, it is assumed that a spatially continuous noise-free set of measurements are available, providing error-free modal information. This case is included to demonstrate how well the identification procedure works under ideal circumstances. To calculate the error coefficients, $\phi_r(x)$ is replaced by $\theta_r(x)$ in Eq. (53).

In Fig. 1, the error coefficients are plotted when all the postulated modes are transformed, as well as in cases when a reduced number of postulated modes are rotated. We observe that the identification results are excellent when all the postulated modes are transformed, thus corroborating the results of Ref. 1. However, when a reduced-order model is used, deterioration in the identification of the higher modes is observed. This is to be expected because the identification procedure cannot diagonalize C_{MM} in Eq. (24), since it is not a unitary matrix. In addition, there is contamination from the residual modes. The nonuniformity in the plot when all modes are transformed is due to numerical inaccuracies.

Case 2

Here, we consider the same actual model as in case 1, but we use discrete sensors and add noise to the system measurements. Modal filters are used to extract the modal quantities from the sensor output. Rayleigh-Ritz type of interpolation functions are chosen,[19] which require that the number of sensors has to be equal to the number of monitored modes.

Figures 2 and 3 compare the performance of the identification procedure for the cases of 12 and 14 sensors. As expected, reducing the number of sensors and the number of transformed modes deteriorates the identification procedure. However, in Fig. 2, we observe that when 12 modes are transformed, the identification results are poor for the higher modes. This is because errors in modal filtering begin to contaminate the identification.

Case 3

The model is the actual one, where 20 modes are used in the system description. It is assumed that a spatially continuously distributed set of measurements is available. This case is similar to case 1, with the exception of the actual model used. The results of this case indicate the degradation due to having a finite-dimensional discretized model.

Figure 4 compares the error coefficients when a discretized postulated model is used of order 15 where, as trial functions, the first set (sinusoidals) are employed. Figure 5 does the same when the second set of trial functions (polynomials) are used to construct the postulated model.

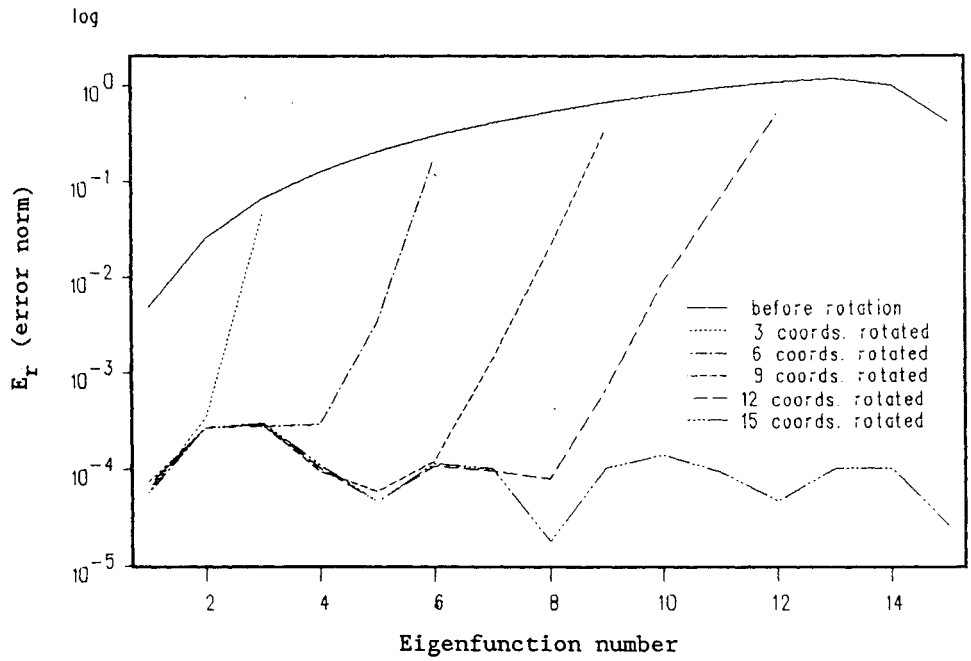

Fig. 1 Ideal case.

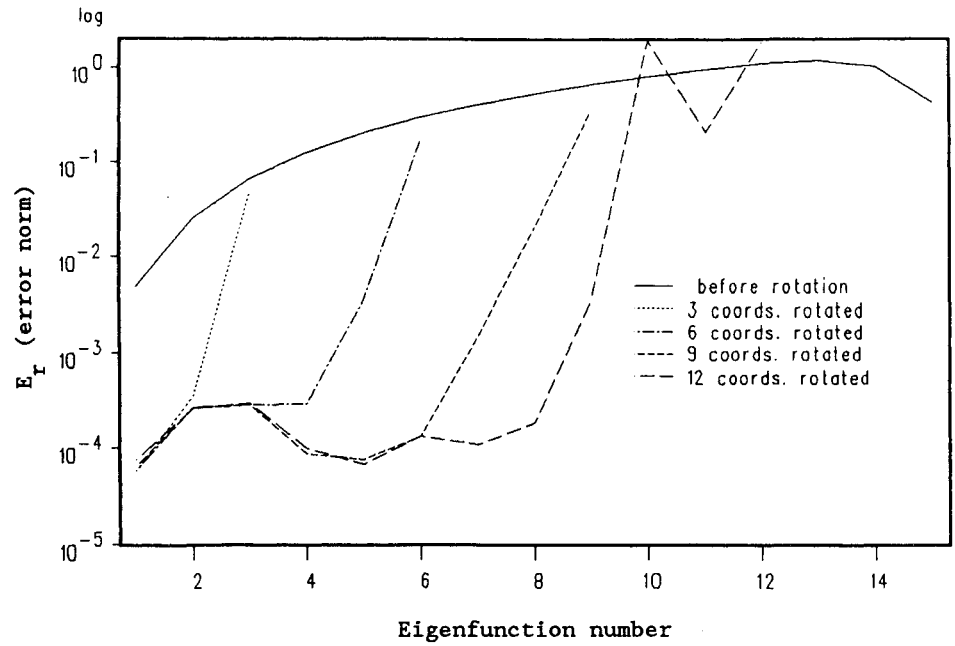

Fig. 2 Fifteen discretized coordinates, 12 sensors.

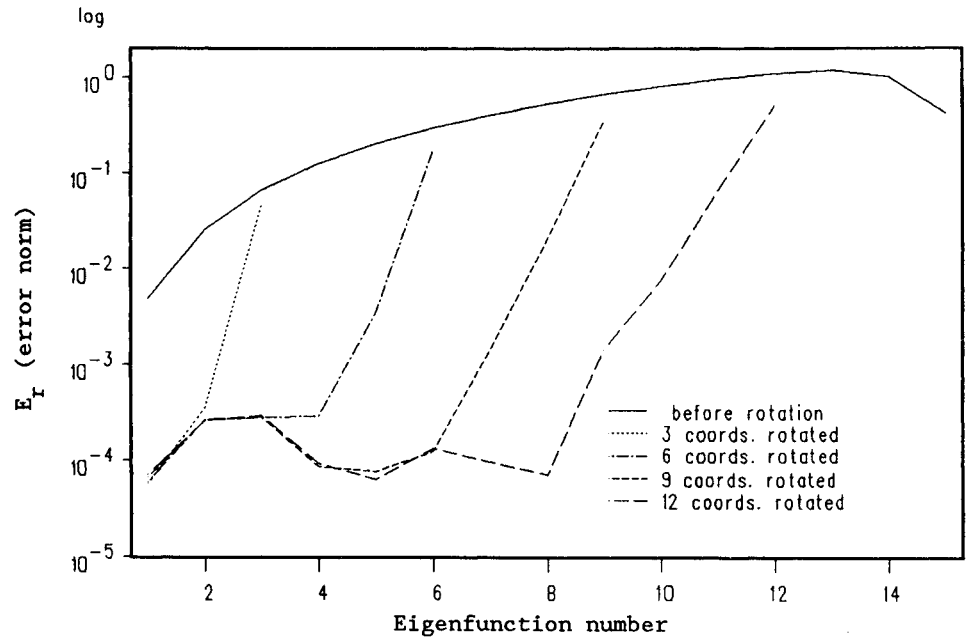

Fig. 3 Fifteen discretized coordinates, 14 sensors.

When comparing Figs. 4 and 5, we observe an interesting phenomenon. When three or six modes are transformed, the accuracy obtained using sinusoidal functions and Chebyshev polynomials are similar. When nine modes are transformed, the polynomials yield better results, and when 12 or all 15 modes are transformed, sinusoidals yield better results. The question arises as to why in some cases sinusoids yield poorer results, considering that the D matrix is much more diagonally dominant when sinusoidals are used as trial functions. The answer lies in the nature of the C matrix. For this particular example, it turns out that the C matrix is more diagonally dominant for polynomial trial functions. When nine modes are transformed, the major source of error is the nonunitariness of the C_{MM} matrix. As the number of transformed modes is increased, errors associated with the spatial discretization dominate, which leads to more accurate results of sinusoidal trial functions.

The above observations lead to two important guidelines. First, the postulated stiffness distribution has to be a logical one. If any function is used to represent the system stiffness, without regard to the nature of the structure, the C matrix will not be diagonally dominant, leading to larger errors when a low number of modes are rotated. Second, regardless of the discretization error, it is recommended to transform as many modes as possible. Then, one can use a limited set of the identified modes as the accurate ones.

Note that whereas in the ideal examples of Ref. 1 any postulated stiffness gives the same result, because of the sources of error described above, the initial estimate affects the accuracy of the results, especially when the number of transformed modes is less than the order of the discretized system.

Case 4

This is the same model as case 3, with the addition of discrete measurements, which are processed by modal filters. Figures 6-9 plot the error coefficients for varying numbers of

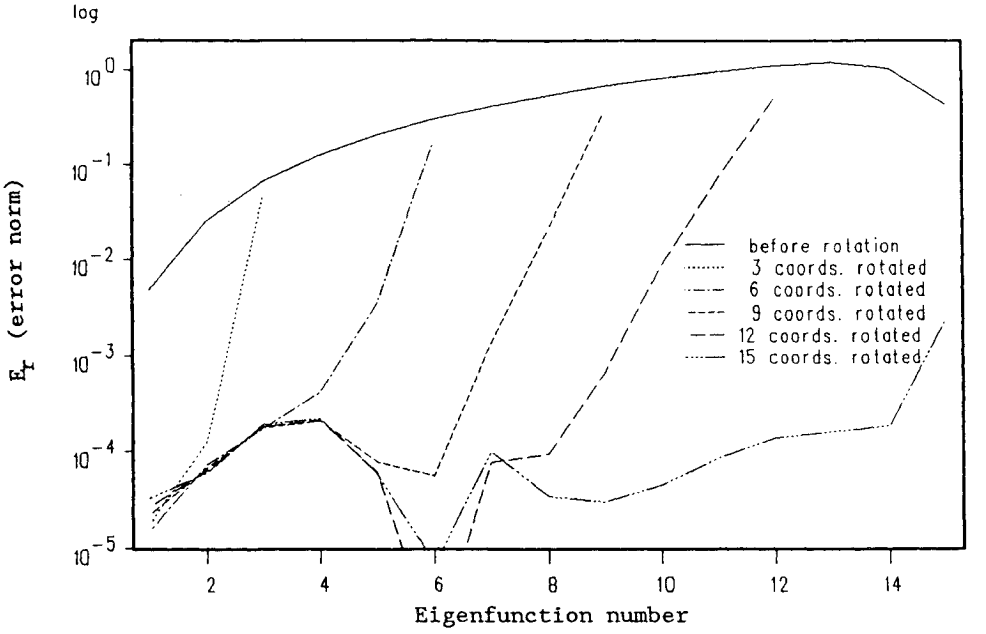

Fig. 4 Fifteen discretized coordinates (sinusoidals).

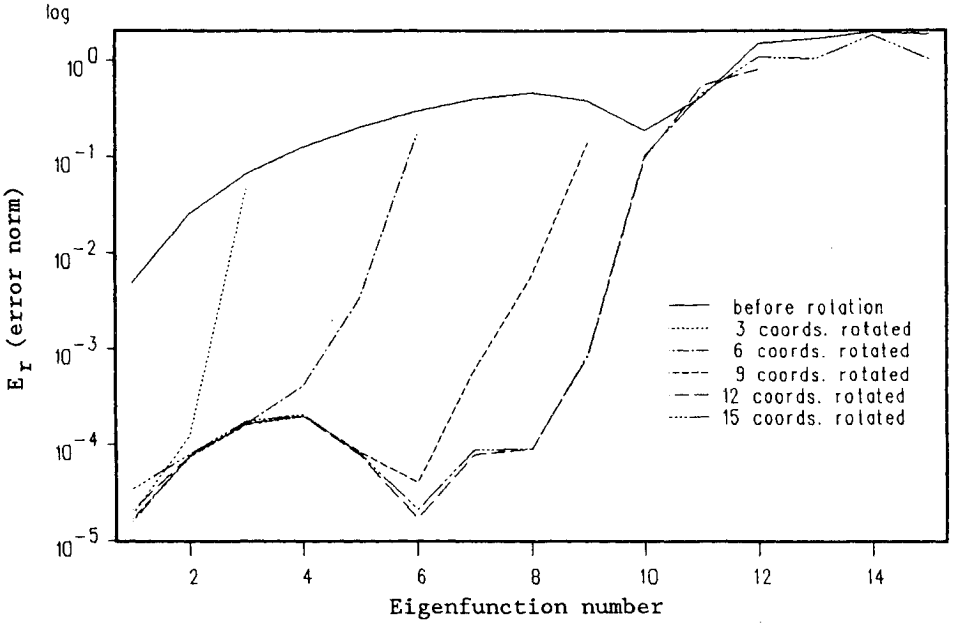

Fig. 5 Fifteen discretized coordinates (polynomials).

sensors, Figs. 6 and 7 use sinusoids as trial functions, and Figs. 8 and 9 use Chebyshev polynomials. As expected, the results show degradation from the results of case 3.

The results in Fig. 8 for the cases of 9 and 12 transformed modes are particularly interesting. The seesawing behavior is observed to be a result of the variation in the degree of contamination imposed by the combined effects of parameter uncertainties, discretization, and modal filtering. When the higher modes are included in the rotations, the C matrix becomes nearly diagonal, while the effects of discretization and modal filtering dominate. However, the points of transition are not the same.

Next, we investigate the consequences of identifying the modes when the underlying assumptions of a damped-free system and accurate mass information are invalid. We analyze how well the identification method, which is based on an undamped model and no mass uncertainties, performs when the actual model is damped and the mass properties are not well known.

Case 5

We assume the uncertainty in the mass distribution to be in the form

$$m'(x) = (1 - e)m(x) \tag{54}$$

where e is an error parameter, and then conduct the identification for various degrees of error. Figure 10 compares the results of the identification when the same model as case 1 is used, for $e = 0.00$, 0.05, and 0.1. As expected, the identification results are deteriorated, however, we observe that even for the case of $e = 0.10$, the error norm of all modes is below 10^{-2}, which is equivalent to a 1% error in the identified eigenfunctions. Note that for this case, because the identified eigenfunctions are not orthogonal with respect to the actual mass distribution, a modified error criterion was introduced and defined as

$$e_r = [\delta_r(x), \delta_r(x)]/[\theta_r(x), \theta_r(x)] \tag{55}$$

Case 6

Here, we consider that the structure is lightly damped and conduct the identification for various amounts of damping. The damping ratios ξ are taken as the same for each mode. Figure 11 compares the results of the identification for three levels of damping: $= 0.00, 0.001, 0.01$. For $\xi = 0.001$, the results of the identification compare favorably with the undamped results. When damping is increased to 0.01, some small deterioration in the accuracy of the identified eigenfunctions is observed.

Finally, we consider implementation problems associated with the identification method used above. If there are periodic external excitations whose frequencies are not known, one may use the peaks associated with these excitations instead of the peaks related to the natural frequencies. The identification procedure in such cases will not converge. The rotation angles may become infinitesimally small, but the peaks in the frequency spectrum will not be minimized. To illustrate this, consider a system of order two, subjected to an excitation of frequency Ω, with the modal responses having the form

$$q_1(t) = 2A_1 \cos\omega_1 t + 2B_1 \cos\Omega t$$

$$q_2(t) = 2A_2 \cos\omega_2 t + 2B_2 \cos\Omega t \tag{56}$$

where A_1, A_2, B_1, and B_2 are constants depending on the initial conditions and magnitude of excitation. Now assume a postulated system related to the actual one, with the unitary transformation

$$q_1'(t) = \cos\alpha q_1(t) + \sin\alpha q_2(t)$$

$$q_2'(t) = \sin\alpha q_1(t) + \cos\alpha q_2(t) \tag{57}$$

so that the actual system can be identified by using a rotation angle $-\alpha$. Introducing Eqs. (56) into Eqs. (57) and taking the

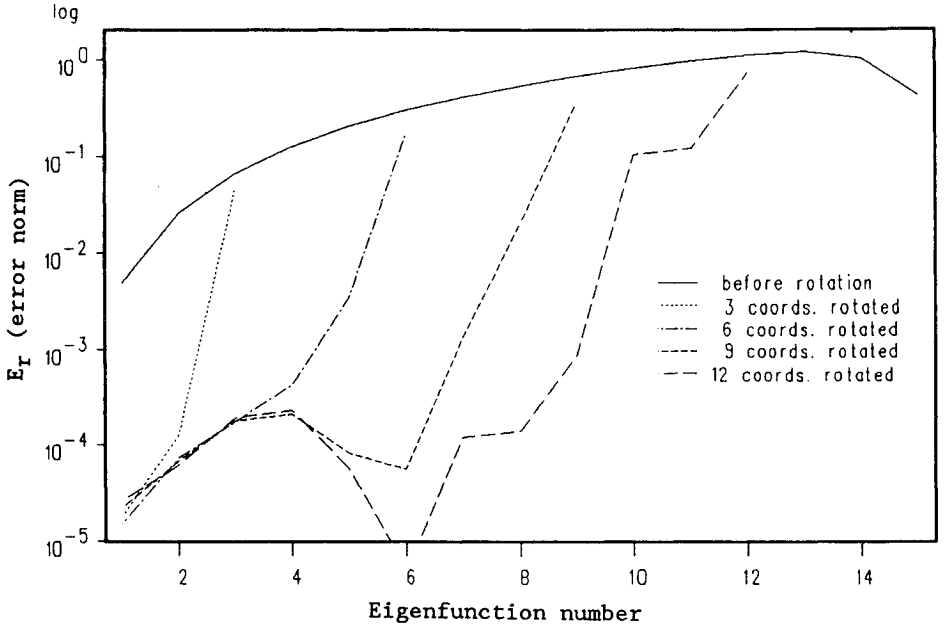

Fig. 6 Fifteen discretized coordinates, 12 sensors (polynomials).

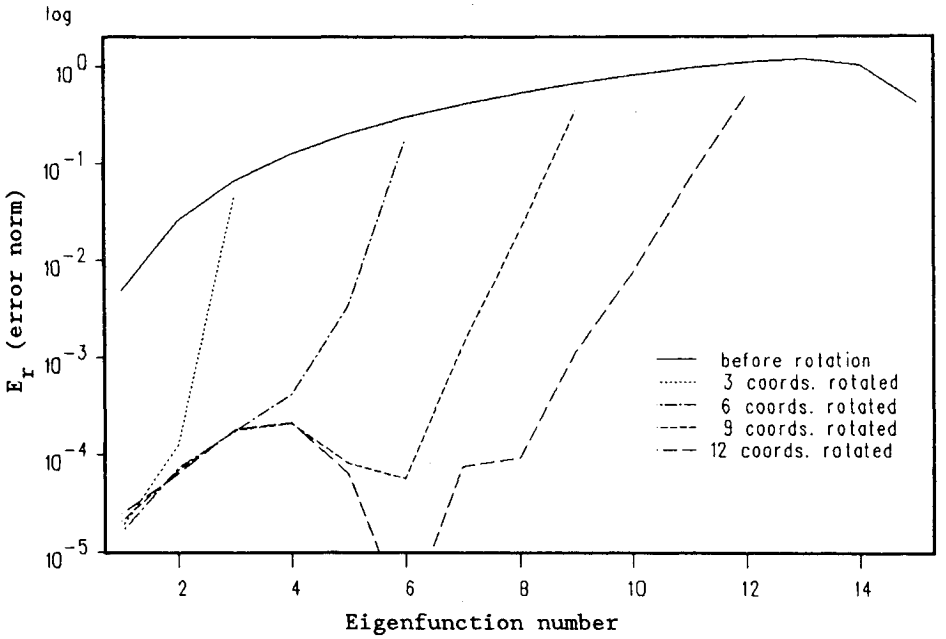

Fig. 7 Fifteen discretized coordinates, 14 sensors (sinusoidals).

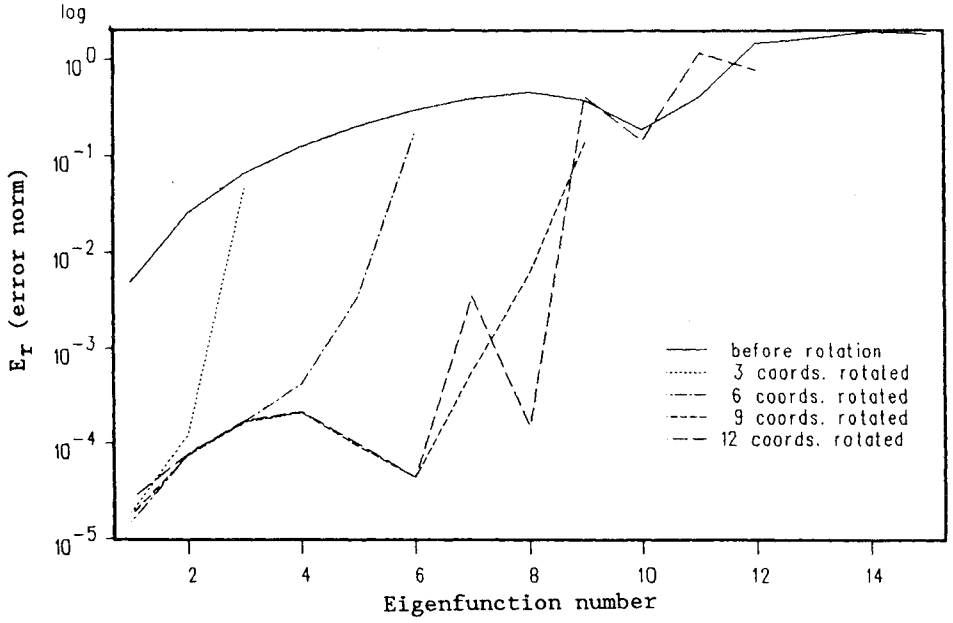

Fig. 8 Fifteen discretized coordinates, 12 sensors (polynomials).

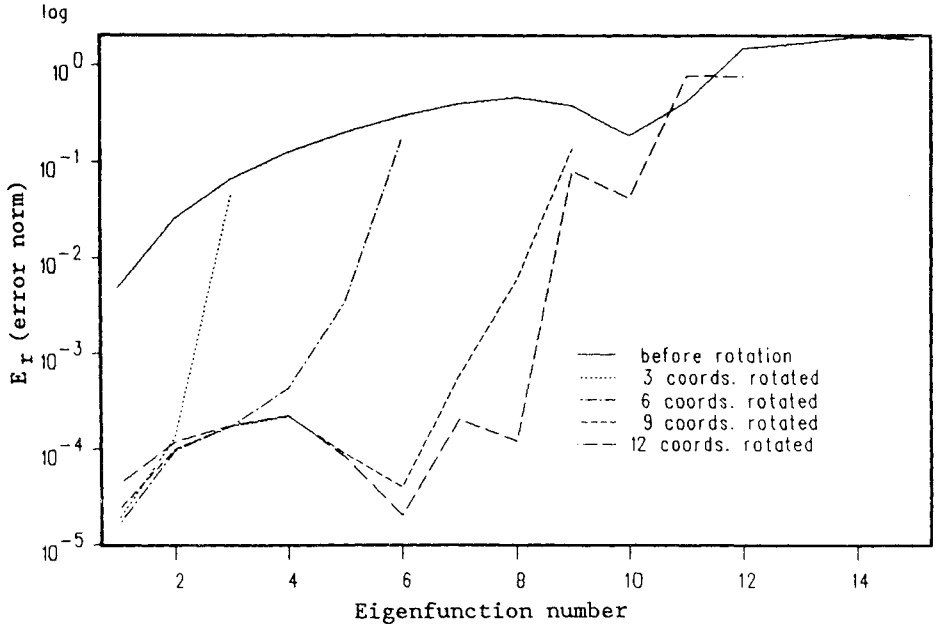

Fig. 9 Fifteen discretized coordinates, 14 sensors (polynomials).

Fourier transform we obtain

$$Q_1'(\omega) = A_1 \cos\alpha\, \delta(\omega - \omega_1) + A_2 \sin\alpha\, \delta(\omega - \omega_2)$$
$$+ (B_1 \cos\alpha + B_2 \sin\alpha)\, \delta(\delta - \Omega)$$
$$Q_2'(\omega) = -A_1 \sin\alpha\, \delta(\omega - \omega_1) + A_2 \cos\alpha\, \delta(\omega - \omega_2)$$
$$+ (B_2 \cos\alpha - B_1 \sin\alpha)\, \delta(\omega - \Omega) \tag{58}$$

where we observe that each postulated mode has three peaks. Now, if one by mistake takes ω_1 and Ω as the modal frequencies, the rotation angle, determined by Eq. (46), will be

$$\tan 2\theta = \frac{2[-A_1^2 \cos\alpha \sin\alpha - (B_2 \cos\alpha - B_1 \sin\alpha)(B_1 \sin\alpha + B_2 \cos\alpha)]}{A_1^2 \cos^2\alpha + (B_2 \cos\alpha - B_1 \sin\alpha)^2 - A_1^2 \sin^2\alpha - (B_1 \cos\alpha + B_2 \sin\alpha)^2} \tag{59}$$

which is not equal to $\tan(-2\alpha)$. It follows that after one rotation there will be no more rotation angles possible, with $q_1^{(2)}(t)$ and $q_2^{(2)}(t)$ still having contributions from three sinusoids. It is therefore very important that the frequencies associated with any periodic excitation be detected and eliminated from the identification procedure. Note that in the above example, $\tan 2\theta$ in Eq. (59) will be equal to $\tan(-2\alpha)$ only if one of B_1 or B_2 is zero, which is impossible. A periodic excitation affects all the modes unless the source of excitation is located at one of the nodes of a certain mode.

We propose a quantitative approach to identify the excitation peaks. The approach is based on a sequential transformation of the coordinates. That is, we first rotate ℓ postulated modal coordinates, where ℓ is much less than n or m. Denoting by Q_{rs} the magnitude of the sth peak in the rth mode, if after the first peaks are transformed, such that the rotation angles become zero, the terms $Q_{rs}(r,s = 1, 2, \ldots, \ell;\ r \neq s)$ are not very much smaller than Q_{rr}, we conclude that the row and column in the matrix $Q(Q = Q_{rs},\ r,s = 1, 2, \ldots, n)$ with the

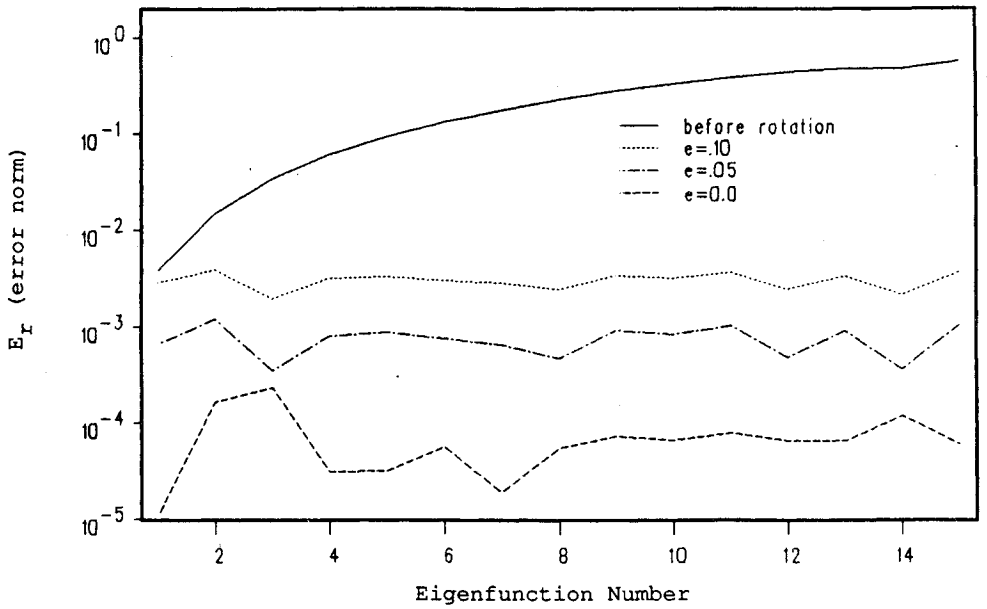

Fig. 10 Effects of uncertainties in the mass distribution.

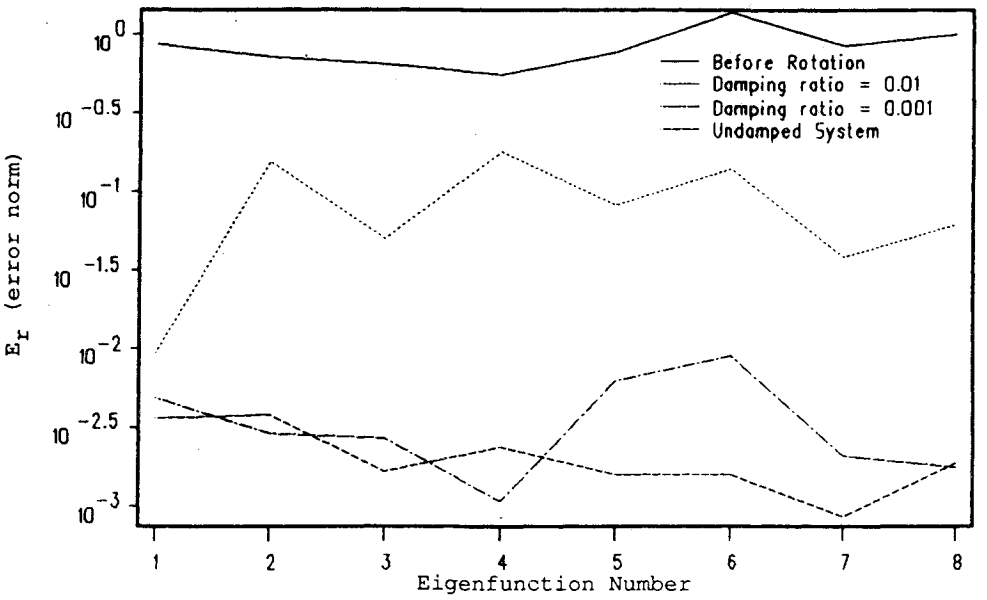

Fig. 11 Effects of damping in the system model.

largest number of off-diagonal terms belonging to an external excitation.

Once a frequency belonging to the external excitations is isolated, it is then removed from the set of rotated modes. The next f peaks are then considered, and the coordinate transformation is carried out for the $\ell+f-1$ postulated modes.

To illustrate the procedure, we use the same model as in case 2. Denoting the frequencies associated with the external excitation by $\Omega_1, \Omega_2, \ldots, \Omega_5$, we select them such that the peaks are ordered as $\omega_1, \Omega_1, \omega_2, \Omega_2, \omega_3, \Omega_3, \omega_4, \Omega_4, \omega_5, \Omega_5, \omega_6, \omega_7, \ldots, \omega_n$.

Table 1 shows the Q matrix after the first four peaks are transformed. For reasons of accuracy we consider the first three rows and columns. Clearly, the second row and column of Q are fully populated, indicating that the second peak does not belong to a system mode. Removing it from the set of modes and including the next peak, which belongs to the third mode, yields the Q matrix given in Table 2.

The peaks now belong to $\omega_1, \omega_2, \Omega_2$, and ω_3. As can be seen, no conclusion can be drawn. We assume that the four peaks are accurate, and increase the number of peaks to be trans-

Table 1 Q Matrix with $\omega_1, \Omega_1, \omega_2, \Omega_2$

41.5304	2.7613	0.7723	2.9778
0.0580	0.8088	0.0993	0.0900
0.5596	3.3198	28.4315	8.9722
3.4903	0.4602	16.3166	48.5384

Table 2 Q Matrix with $\omega_1, \omega_2, \Omega_2, \omega_3$

41.4864	1.4146	3.4272	1.4069
0.8246	23.8292	10.3297	6.7116
3.7694	19.7493	45.5631	22.1945
1.1201	9.1480	15.8397	32.5248

Table 3 Q Matrix with $\omega_1, \omega_2, \Omega_2, \omega_3, \Omega_3, \omega_4$

41.4808	1.6371	3.3901	1.4670	4.2487	0.7378
0.8819	22.0996	10.1241	6.5842	9.4849	4.1916
3.7755	21.1222	46.1587	22.9601	0.9487	6.0167
1.2104	10.0273	16.7617	33.7054	0.1388	3.1677
0.3341	1.3914	0.0812	0.0431	3.1927	1.8482
0.3030	3.1152	2.1489	1.5554	9.5718	16.5450

Table 4 Q **Matrix with** ω_1, ω_2, ω_3, Ω_3, ω_4, Ω_4

41.6763	0.1097	0.1670	3.9384	0.0805	0.8425
0.0719	32.3706	0.5676	6.5941	0.4126	0.7701
0.3203	0.1553	41.3604	1.8228	0.7382	1.3316
0.5626	1.2066	0.2610	5.9220	3.4830	2.1148
0.1191	0.2407	0.2960	10.6399	18.1275	3.4988
0.0223	0.0283	0.0490	0.3932	0.2270	1.1015

formed to six. The resulting Q matrix is shown in Table 3. Considering the first four rows and columns, we observe that the populated ones belong to the second and third peaks. We next compare Q when we remove the second row and column to the case where we remove the third row and column. The results clearly indicate that the third row and column, which correspond to Ω_2, should be removed. Eliminating the third peak, and adding the next peak, so that the peaks in consideration now belong to ω_1, ω_2, ω_3, Ω_3, ω_4, Ω_4, we rotate. The results are shown in Table 4. The procedure is continued until all the excitation peaks are eliminated.

VI. Conclusions

Issues associated with real-time implementation of modal identification methods are discussed. It is shown that the accuracy of the identification is deteriorated by using discrete point sensors and because the mathematical model is finite-dimensional and spatially discretized. The individual and combined effects of spatial discretization, reduced-order modeling, and point sensors are qualitatively and quantitatively investigated. It is concluded that errors due to reduced-order modeling dominate the degradation of the accuracy of the identification. It is thus recommended to retain as many of the higher modes as possible in the model during identification.

Acknowledgment

The research reported herein has been supported in part by the National Science Foundation under Grant NSF MEA-85-01877.

References

[1]Baruh, H., and Khatri, H. P., "Identification of Modal Parameters in Vibrating Structures," *Journal of Sound and Vibration,* Vol. 125, No. 3, 1988, pp. 413–427.

[2]Berman, A., "Parameter Identification Techniques for Vibrating Structures," *Shock and Vibration Digest,* Vol. 11, No. 1, 1979.

[3]Strejc, V., "Trends in Identification," *Automatica,* Vol. 17, No. 1, 1981, pp. 7–21.

[4]Kubrusly, C. S., "Distributed Parameter Identification, a Survey," *International Journal of Control,* Vol. 26, No. 4, 1977, pp. 509–535.

[5]Ljung, L., and Glover, K., "Frequency Domain Versus Time Domain Methods in System Identification," *Automatica,* Vol. 17, No. 1, 1981, pp. 71–86.

[6]Banks, H. T., and Crowley, J. M., "Parameter Identification in Continuum Models," *Journal of the Astronautical Sciences,* Vol. 33, No. 1, 1985, pp. 85–94.

[7]Bergman, L. A., Hale, A. L., and Gooding, J. C., "Identification of Linear Systems by Poisson Moment Functionals in the Presence of Noise," *AIAA Journal,* Vol. 23, No. 8, 1985, pp. 1234, 1235.

[8]Caesar, B., and Peter, J., "Direct Update of Dynamic Mathematical Models from Modal Test Data," *AIAA Journal,* Vol. 25, No. 11, 1987, pp. 1494–1499.

[9]Caravani, P., and Thomson, W. T., "Identification of Damping Coefficients in Multidimensional Linear Systems," *Journal of Applied Mechanics,* Vol. 41, No. 1, 1974, pp. 379–382.

[10]Ibrahim, S. R., "Computation of Normal Modes from Identified Complex Modes," *AIAA Journal,* Vol. 21, No. 3, 1983, pp. 446–451.

[11]Ewins, D. J., and Gleeson, P. T., "A Method for Modal Identification in Lightly Damped Structures," *Journal of Sound and Vibration,* Vol. 84, No. 1, 1982, pp. 57–79.

[12]Juang, J.-N., and Pappa, R. S., "An Eigensystem Realization Algorithm for Modal Parameter Identification," *Journal of Guidance, Control, and Dynamics,* Vol. 9, No. 5, 1985, pp. 620–627.

[13]Baruh, H., and Meirovitch, L., "Parameter Identification in Distributed Systems," *Journal of Sound and Vibration,* Vol. 101, No. 4, 1985, pp. 551–564.

[14]Baruch, M., "Correction of Stiffness Matrix Using Vibration Tests," *AIAA Journal,* Vol. 20, No. 3, 1982, pp. 441, 442.

[15]Berman, A., "Mass Matrix Correction Using an Incomplete Set of Measured Modes," *AIAA Journal,* Vol. 17, No. 10, 1979, pp. 1147, 1148.

[16]Kabe, A. M., "Stiffness Matrix Adjustment Using Mode Data," *AIAA Journal,* Vol. 23, No. 10, 1985, pp. 1431–1436.

[17]Beliveau, J. G., "Identification by Viscous Damping in Structures from Modal Information," *Journal of Applied Mechanics,* Vol. 43, No. 2, 1976, pp. 335–339.

[18]Baruh, H., and Silverberg, L., "Identification of External Excitations in Self-Adjoint Systems Using Modal Filters," *Journal of Sound and Vibration,* Vol. 108, No. 2, 1986, pp. 247–260.

[19]Meirovitch, L., and Baruh, H., "Implementation of Modal Filters for Control of Structures," *Journal of Guidance, Control, and Dynamics,* Vol. 8, No. 6, 1985, pp. 707–716.

[20]Baruh, H., and Choe, K., "Sensor Failure Detection Method for Flexible Structures," *Journal of Guidance, Control, and Dynamics,* Vol. 10, No. 5, 1987, pp. 474–482.

[21]Meirovitch, L., *Computational Methods in Structural Dynamics,* Sijthoff & Noordhoff, Alpen aan den Rijn, The Netherlands, 1980.

[22]Baruh, H., and Boka, J., "Model Parameter Identification in Space Structures," *Proceedings of the USAF NASA Workshop on Model Determination for Large Structures,* March 22–24, 1988, Pasadena, CA, pp. 97–116.

[23]Brigham, E. O., *The Fast Fourier Transform,* Prentice-Hall, Englewood Cliffs, NJ, 1974.